SYNOPTIC-MESOSCALE ANALYSIS OF THE FLASH-FLOOD-PRODUCING THUNDERSTORM OVER THE VALLÉE DE L'ERNZ ON 22 JULY 2016

Date	**12/04/2021**
Author	**Luca Mathias**
Version	**2.0**
Number of pages	**16**

TABLE OF CONTENTS

1. INTRODUCTION 3
2. DATA 4
3. OVERVIEW OF THE ATMOSPHERIC CONDITIONS 5
4. STORM CELL ANALYSIS 8
5. PRECIPITATION ANALYSIS 11
6. SUMMARY AND CONCLUSIONS 13
ACKNOWLEDGEMENTS 13
REFERENCES 14

1. INTRODUCTION

On 22 July 2016, the Vallée de l'Ernz in the eastern part of Luxembourg was hit by torrential convective rainfall that triggered catastrophic flash floods during the evening hours, accounting for substantial damage in the amount of at least 6 million Euros. According to eyewitness reports in several media the flash floods in the Vallée de l'Ernz started at different times along the valley, with an approximate time frame from 18:15 to 19:00 UTC. The orography of the Vallée de l'Ernz and Larochette is dominated by a north-south orientated river valley with altitudes of 240 to 270 m, surrounded by a hilly landscape with altitudes up to 420 m and steep slopes, especially between Medernach and Larochette (Fig. 1). The river White Ernz (fr. Ernz Blanche) flowing through the towns of Ermsdorf, Medernach and Larochette (Fig. 1) reached a maximum water level of 175.9 cm in Larochette (Pfister et al. 2018). It was one of the most severe hydro-meteorological events in the Luxembourgish territory in the last decades and comparable events took place in regions close to the Vallée de l'Ernz on 1 July 1958 (D'Letzeburger Land 1958, Luxemburger Wort 2018) and on 1 June 2018 in the Mullerthal region (Mathias 2019). Pfister et al. (2018) estimated that the precipitation event, which occurred between Larochette and Ermsdorf, has a return of period of more than 100 years.

The aforementioned characteristics of this event motivate a detailed investigation. This case study is focused on the meteorological features of this hazardous weather event, with the following main objectives:

- To identify the atmospheric synoptic-scale and mesoscale conditions that favoured the development of this extreme rainfall event.
- To examine the development of the flash-flood-producing thunderstorm.
- To provide a spatial and temporal analysis of the precipitation that triggered the flash floods and landslides.

This article is structured as follows: Section 2 describes the data used in this study and an overview of the atmospheric conditions will be provided in section 3. An analysis of the flood-producing storm is given in section 4 and the precipitation observations are examined and discussed in section 5. The last section includes a short summary and the conclusions.

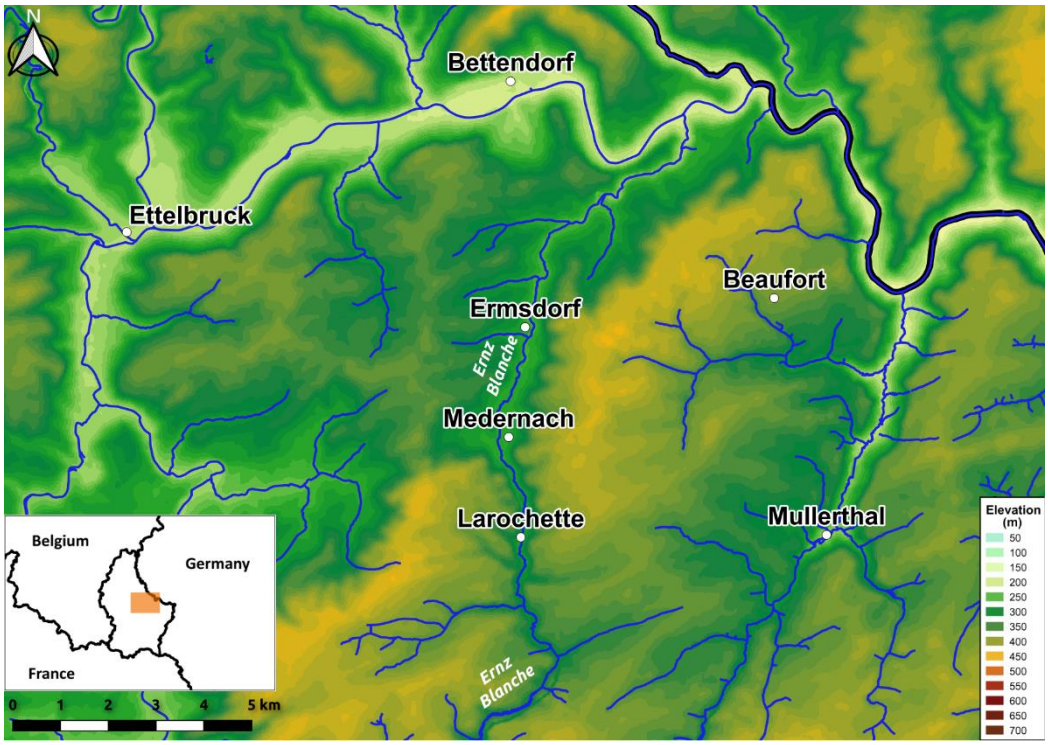

Figure 1. Topographic map of the investigation area (shaded orange in the inset on the lower-left-hand side).

2. DATA

ERA5 reanalysis data from the European Centre for Medium-Range Weather Forecasts (ECMWF) will be used to examine the synoptic-scale conditions. ERA5 was produced using 4D-Var data assimilation with the model cycle 41r2 of ECMWF's Integrated Forecast System (IFS). The hourly reanalysis data output has a native horizontal grid spacing of 31 km and 137 levels in the vertical (Hersbach et al. 2020). The storm cell analysis will be based on the low-level precipitation scan of the C-band radar in Neuheilenbach, which is operated by the German Weather Service (Deutscher Wetterdienst; DWD). The scan has a horizontal resolution of 250 m in range and a maximum range of 150 km. The data is visualised by the Kachelmann Group (2021). In addition to the radar data, lightning data from nowcast (Betz et al. 2009) will be considered. The in situ measurements of precipitation include data from the surface weather station network operated by the meteorological department[1] of the Administration des Services Techniques de l'Agriculture (ASTA). The data has a temporal resolution of 10 minutes. Moreover, 5-minute data from the radar-based precipitation climatology project of the DWD (RADKLIM; Winterrath et al. 2017), which uses the quantitative precipitation estimation method RADar-OnLine-ANeichung (RADOLAN; Bartels et al. 2004), will be analysed as well. The RADKLIM data has a grid interval of 1 km.

[1] https://www.agrimeteo.lu/

3. OVERVIEW OF THE ATMOSPHERIC CONDITIONS

On 22 July 2016, a meridional circulation was active in the upper troposphere over Western Europe. At 15:00 UTC, an upper-level trough was located over England, western France, and the Iberian Peninsula, exhibiting asymmetric structures and a vorticity streamer in 300 hPa extending from Iceland to eastern Spain (Fig. 2a). On its rear side, a jet stream with wind speeds exceeding 40 m s^{-1} was present over the Bay of Biscay and Spain (Fig. 2a). The front side of the long-wave trough was more diffuse with weaker geopotential and temperature gradients. Hence, the southerly upper-tropospheric flow was weak over eastern France, western Germany, and Benelux. However, a small and anticyclonically curved jet streak with a local wind maximum of 30 m s^{-1} was situated over Belgium and southern Netherlands (Fig. 2a). As the flow curvature in 300 hPa remained anticyclonic due to the persistence of the upper-level ridge over eastern Germany and in combination with a nearly straight flow in 500 hPa (Fig. 2a), no significant large-scale forcing for ascent was identifiable over the Greater Region.

The examination of the low-level conditions was challenging due to a weak pressure gradient over Central Europe. Indeed, the 12:00 UTC surface analysis from three meteorological services (German Weather Service, United Kingdom Meteorological Office, and Royal Netherlands Meteorological Institute) resulted in three different interpretations (not shown). Based on ERA5 reanalysis data, an ill-defined and wavy zone with temperature and moisture gradients extended from France to the North Sea (Fig. 2b), separating subtropical air masses in the east from heated maritime polar air masses west of this front-like gradient zone. Moreover, a strong moisture gradient was evident over north-eastern Germany, and a bow-shaped low-level convergence zone was situated over northern Germany (Fig. 2b). The surface pressure distribution revealed a weak low-pressure area with embedded convergence zones over the Greater Region and southern Germany at 15:00 UTC (Fig. 2b), which remained amorphous until the evening hours, as the ongoing activity of convective storms further significantly affected the conditions near the surface.

Furthermore, high amounts of tropospheric water vapour were observed in the regime of the subtropical air mass over Central Europe, with precipitable water values between 27 and 30 mm over Luxembourg (Figs. 2b). Backward trajectory analyses suggest that the moist air mass was advected from the Bay of Biscay and from the subtropical North Atlantic with a south-westerly flow between 17 July and 21 July 2016 (Fig. 3).

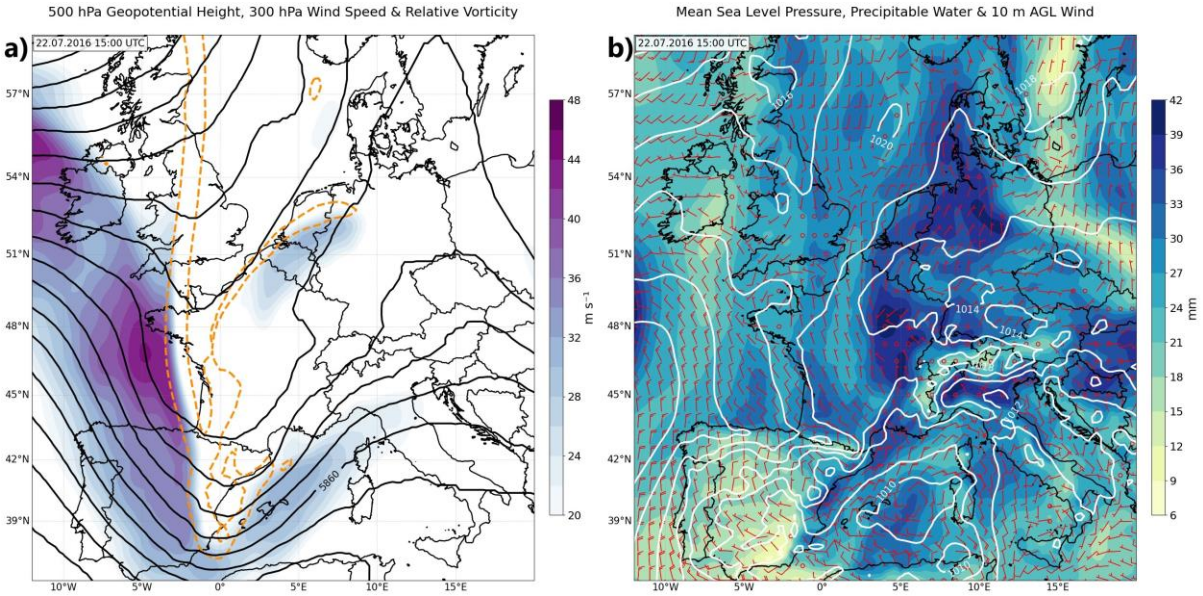

Figure 2. ERA5 reanalysis of the synoptic-scale conditions on 22 July 2016 at 15:00 UTC over Western and Central Europe. (a) 500 hPa geopotential height (black lines; gpm; line spacing is 20 gpm), 300 hPa wind speed (shaded; m s^{-1}) and areas of 300hPa relative vorticity exceeding 0.00015 s^{-1} are denoted by the dashed orange lines. (b) Mean sea level pressure (white lines; hPa), total precipitable water (shaded; mm) and 10 m above ground level (AGL) wind (red barbs; kts).

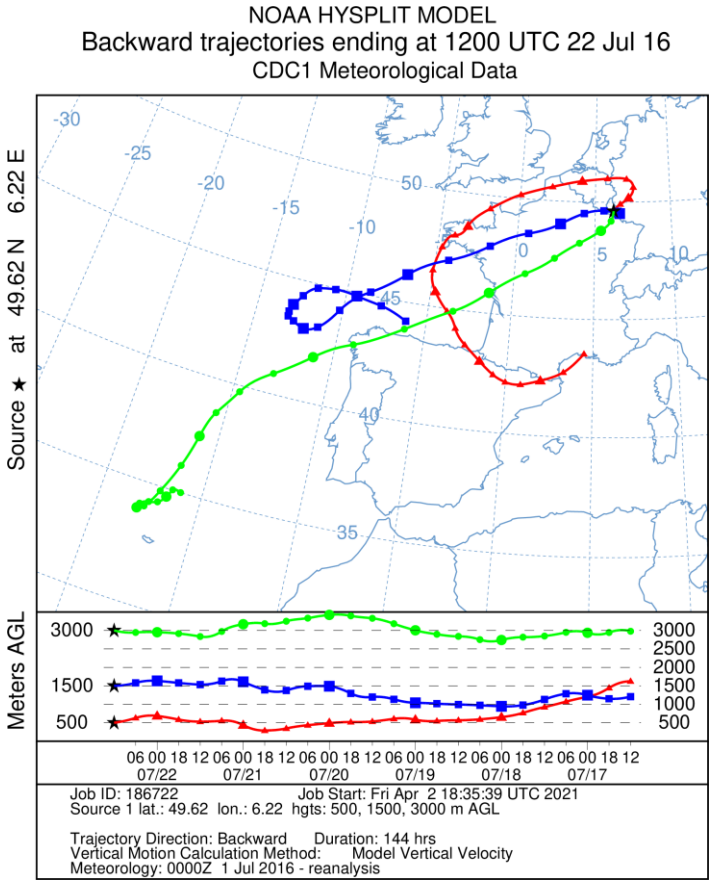

Figure 3. Backward trajectories of air parcels being present at 500 m, 1500 m and 3000 m AGL above Luxembourg. The trajectories were calculated by NOAA's HYSPLIT model (Stein et al. 2015) based on NCEP/NCAR reanalysis data. The trajectory duration is 144 hours (6 days).

The evening sounding from Idar-Oberstein (about 80 km east of the Vallée de l'Ernz) on 22 July 2016 is considered representative of the atmospheric conditions prevailing over Luxembourg due to an easterly flow in the lower troposphere and negligible contamination by convection at that time. The sounding measurements revealed a well-mixed boundary layer up to 850 hPa with a mean mixing ratio of 12.2 g kg^{-1} in the lowest 500 m and a mean relative humidity of 64 % between the surface and 600 hPa (Fig. 4). An elevated mixed layer (EML) was present between 810 hPa and 720 hPa, resulting in lapse rates of 8.3 K km^{-1} between the surface and 3 km AGL (Fig. 4). The combination of a moist boundary layer and steep lower-tropospheric lapse rates resulted in a 500-m mixed-layer (ML) convective available potential energy (CAPE) of about 1500 J kg^{-1}, of which about 600 J kg^{-1} were available within the hail-growth-layer (Fig. 4). The convective inhibition (CIN) was zero, meaning that a near-surface air parcel being lifted would easily reach the level of free convection. The ascending trajectory of both the surface-based (SB) parcel and the mixed-layer parcel also revealed a relatively low lifted condensation level (LCL) at about 1000 m AGL (Fig. 4).

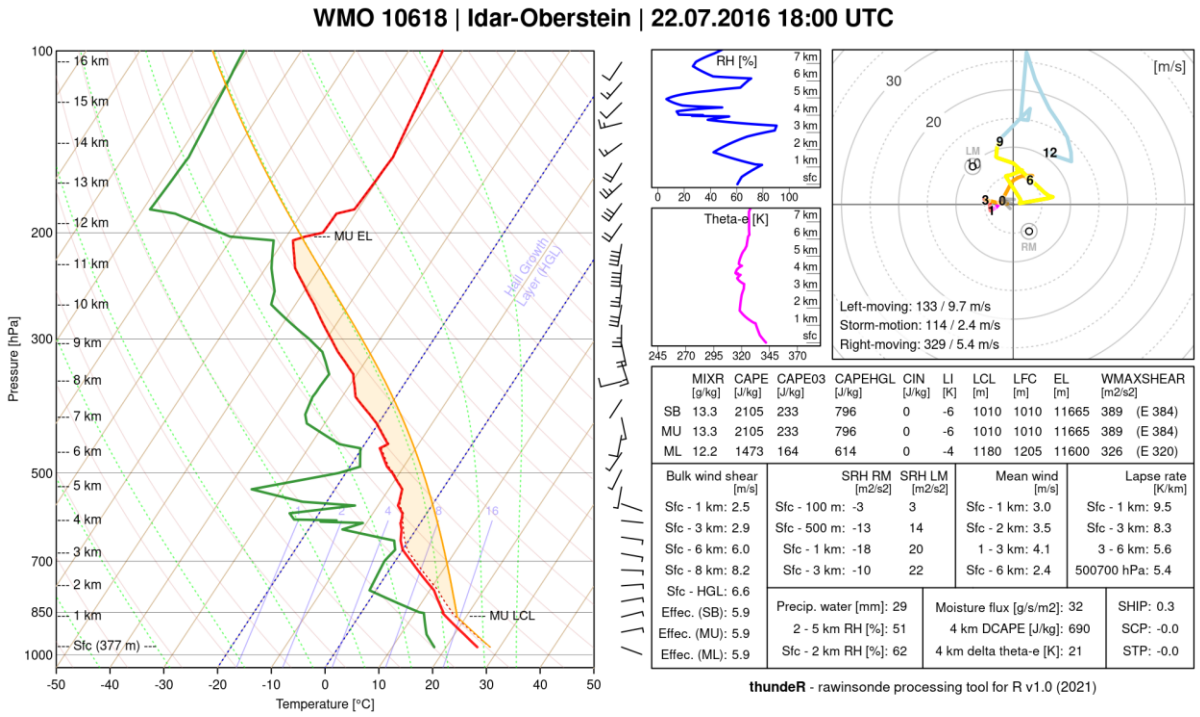

Figure 4. Skew T-log p diagram of a sounding from Idar-Oberstein (WMO 10618) launched at 17:00 UTC on 22 July 2016. The red (green) curve represents the temperature (dew point), and the yellow curve represents the ascent trajectory of the most unstable air parcel. The most-unstable convective available potential energy (CAPE) is indicated by the area shaded in transparent yellow. The lifted condensation level (LCL) marks the expected cloud base of a convective storm. The wind barbs are displayed in knots.

Due to very weak lower- to mid-tropospheric air flow, the vertical wind speed shear between the surface and 6 km AGL remained around 6 m s^{-1} (Fig. 4). Moreover, a mean wind speed of 2.4 m s^{-1} within the same layer hinted at a strongly reduced motion speed of storm cells. However, the speed shear was stronger in the upper troposphere with roughly 20 m s^{-1} between 6 and 11 km AGL (Fig. 4), ensuring some ventilation of the upper part of the storm cloud, which could potentially increase the longevity of the storm's updraft.

In brief, the environment was highly favourable for the development of disorganized deep moist convection (DMC). A high boundary layer moisture, steep lapse rates and weak dynamics characterized the lower troposphere. The forcing to initiate DMC was provided by sub-synoptic-scale processes (e.g., low-level convergence zones, outflow boundaries, boundary layer thermals), but also by forced ascent along the German and Belgian low mountain ranges. This regime of strong latent instability, high total column water vapour, and weak lower-tropospheric kinematics generally allows the formation of slow moving and training thunderstorms which can produce extreme rainfall amounts on the micro-α to meso-γ scale (e.g., Doswell et al. 1996, Púčik et al. 2015, Schumacher 2017).

4. STORM CELL ANALYSIS

On 22 July 2016, the first convective cells appeared over far north-western Luxembourg near the Belgian border at 13:00 UTC, which were initiated by the outflow boundary from convection over the Ardennes (not shown). These weak cells dissolved around 14:00 UTC and at the same time new convective cells formed over Trier. One of these cells moved slightly to the west while strengthening and reached the region of Mertert and Mompach at 15:00 UTC. This storm cell weakened then rapidly until 15:40 UTC, whereas a new thunderstorm developed to the south over Flaxweiler and Grevenmacher in eastern Luxembourg. While this storm cell dissolved until 16:15 UTC, a new convective cell formed between Luxembourg City and Niederanven around 15:55 UTC, which moved slightly to the west and began to weaken at 16:20 UTC. The weather station at the Airport Luxembourg-Findel (located directly southwest of Niederanven) reported an hourly precipitation amount of 29.7 mm between 16:00 and 17:00 UTC (of which 14.6 mm fell within 10 minutes), indicating the potential for high precipitation amounts within a short period of time.

The parent cell of the flash-flood-producing thunderstorm over the Vallée de l'Ernz developed near Consdorf around 17:00 UTC and moved slowly in a westerly direction (Fig. 5a). Furthermore, a multicellular thunderstorm formed directly north of Vianden west of the German city Bitburg between 16:30 and 17:00 UTC. This storm propagated slightly to the south, with the strongest precipitation core located over Fouhren and Longsdorf at 17:30 UTC (feature "1" in Fig. 5a). At the same time, the parent cell rapidly intensified north of Larochette at 17:30 UTC (cf. Figs. 5a with 5b). This storm further strengthened while remaining quasi-stationary over the Vallée de l'Ernz and merged with the storm cell near Longsdorf between 18:00 and 18:15 UTC (cf. Figs. 5a and 5b with 5c). Hence, a heavy thunderstorm extended from Larochette over Nommern and Medernach to Longsdorf at 18:20 UTC. Simultaneously, a single cell storm developed rapidly near Echternach and then moved to the west to merge with the quasi-stationary thunderstorm over the Vallée de l'Ernz at 18:30 UTC (feature "2" in Figs. 5c and 5d). These two feeding processes were likely crucial for the long-lasting intense convective precipitation, since several past studies showed that the merging process often has an intensification effect on the storm development and thus, can significantly enhance the precipitation rate (e.g., Bennetts et al. 1982, Westcott 1984, 1994, Fu and Guo 2006, Fu and Guo 2012, Sinkevich and Krauss 2014, Sinkevich et al. 2018). Finally, the rainfall stopped over the valley of the White Ernz at about 19:30 UTC.

Looking in greater detail at the measured radar pixel values over the Vallée de l'Ernz, local reflectivity maxima of 60 to 63 dBZ were observed over the that area between 18:25 and 18:45 UTC (Figs. 5d and 5e), whereby reflectivity values of 45 to 55 dBZ were present during an entire hour from 17:50 until 18:50 UTC (Fig. 5). This flash-flood-producing storm cell also possessed a vertically stacked reflectivity core with values above 55 dBZ between 18:20 and 18:40 UTC, reaching an altitude of about 8 km (not shown). During that exact period, an impressively high rate of intra-cloud lightning flashes with more than 50 flashes min^{-1} was observed (Fig. 6b). More precisely, three major lightning jumps (i.e., rapid increases in total lightning) were subjectively identified around 18:15 UTC, 18:21 UTC and 18:29 UTC (Fig. 6b). These jumps often indicate the occurrence of severe weather at the ground (Schultz et al. 2011, Jurković et al. 2015, Farnell et al. 2017, Wapler 2017) and they are associated with a growth of the updraft volume and graupel mass in the mixed phase region of the storm cloud (Deierling and Petersen 2008, Schultz et al. 2017). Indeed, the total lightning increase between 18:10 and 18:21 UTC coincides well with the period of the first merging process which took place between Larochette and Longsdorf. Overall, the thunderstorm over the Vallée de l'Ernz produced about 3000 lightning strokes between 17:45 and 19:00 UTC (Fig. 6).

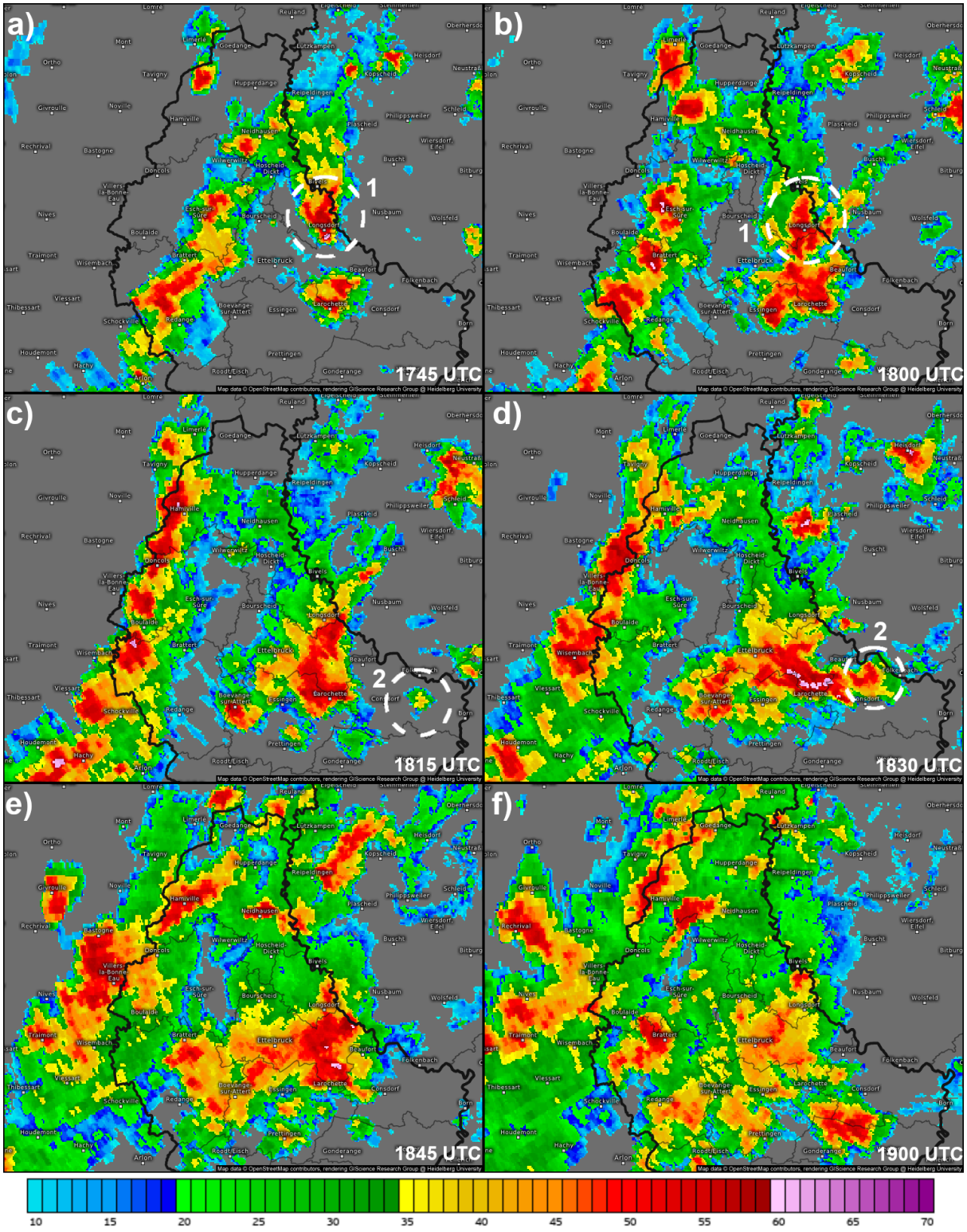

Figure 5. Reflectivity (dBZ) measured at (a) 17:45UTC, (b) 18:00 UTC, (c) 18:15 UTC, (d) 18:30 UTC, (e) 18:45 UTC and (f) 19:00 UTC with an elevation angle of 0.8° by the meteorological radar located in Neuheilenbach to the north-east of the flash-flood-producing storm and operated by the German Weather Service (DWD). The features "1" and "2" in (a)-(d) are quoted in the text. Images are adapted from: https://kachelmannwetter.com/lu/regenradar.

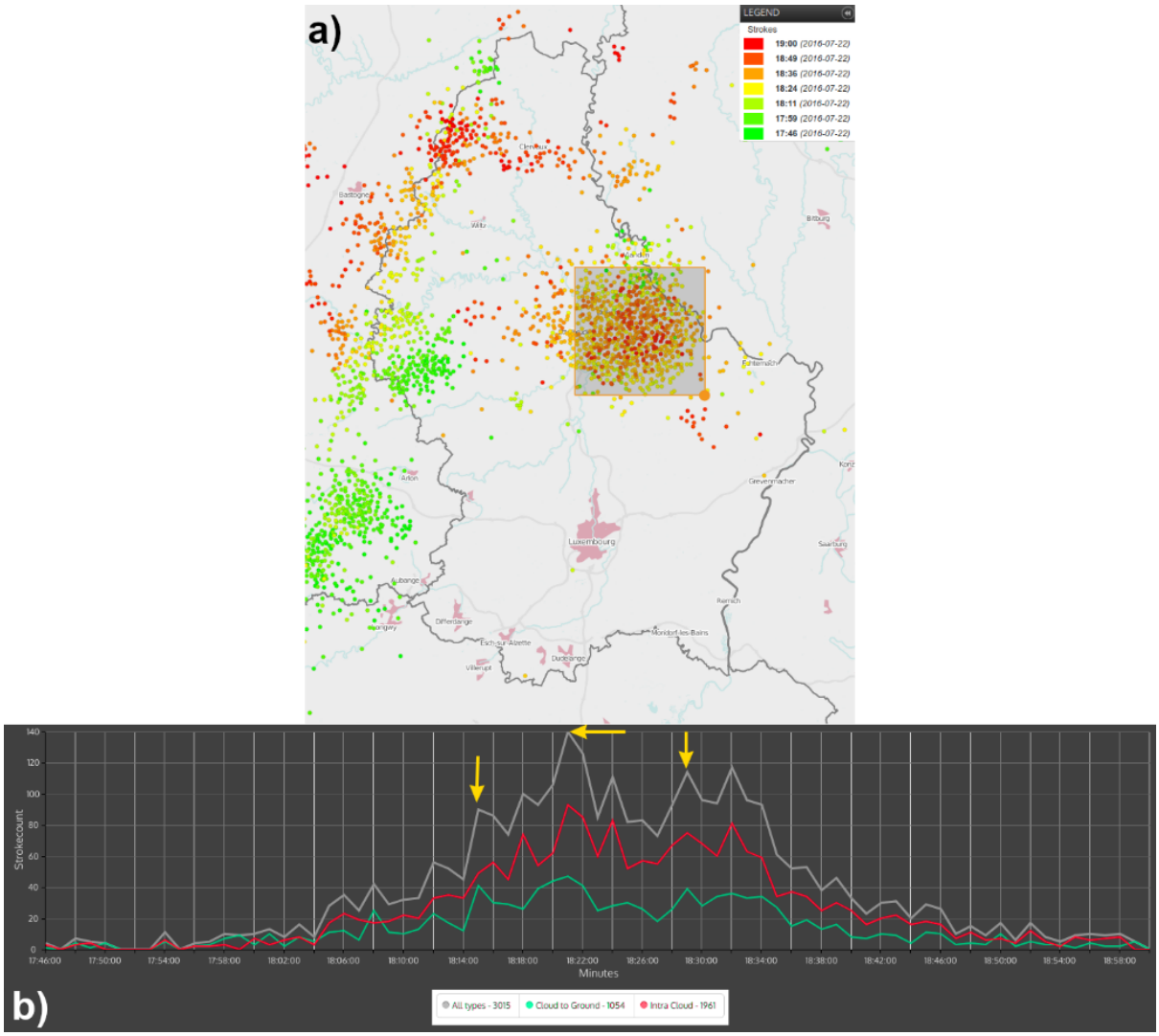

Figure 6. (a) Detected lightning strokes over Luxembourg between 17:45 and 19:00 UTC. (b) Temporal evolution of cloud-to-ground (green line) and intra-cloud (red line) lightning within the area indicated by the greyish box in (a). The yellow arrows in (b) denote the subjectively analysed lightning jumps.

5. PRECIPITATION ANALYSIS

As shown in section 4, long-lasting and intense precipitation rates caused the extreme rainfall amounts over the Vallée de l'Ernz. The RADKLIM precipitation estimates indicated an hourly accumulation of 30 to 50 mm within a broad area between Larochette and Bettendorf for the period 17:50 to 18:50 UTC, especially over the southern part of the White Ernz between Larochette and Ermsdorf, where multiple pixels exceeded 40 mm with a peak value of 51.1 mm (Fig. 7). However, when comparing these pixel values with in situ precipitation data, it becomes evident that RADKLIM underestimated the peak rainfall amounts (Fig. 7). The ASTA weather station in Christnach reported an hourly precipitation amount of 53.1 mm (30.7 mm between 18:10 and 18:30 UTC), whereas the nearest RADKLIM pixel suggested a value of about

17 mm. The underestimation is less pronounced for the area near Stegen, where a private semi-professional weather station even measured 59.6 mm within one hour, while RADKLIM suggested 34 mm (Fig. 7). Since the measurements in Bettendorf coincide well with RADKLIM (Fig. 7) and the precipitation in Christnach was measured at the southern flank of the storm, and thus downstream of the radar beam, strong beam attenuation may have significantly affected the RADKLIM precipitation estimation to the south and west of Ermsdorf. Indeed, Kreklow et al. (2019) outlined that RADKLIM has a negative bias causing an underestimation of extreme precipitation due to rainfall-induced beam attenuation and spatial averaging. Thus, RADKLIM likely underestimated the maximum precipitation amounts between Larochette and Ermsdorf by an approximate factor of 2 (± 0.5). Based on these findings, it can be reliably estimated that precipitation amounts of 60 to 100 mm accumulated within one hour over the southern part of the White Ernz valley, which is supported by the estimations from Pfister et al. (2018).

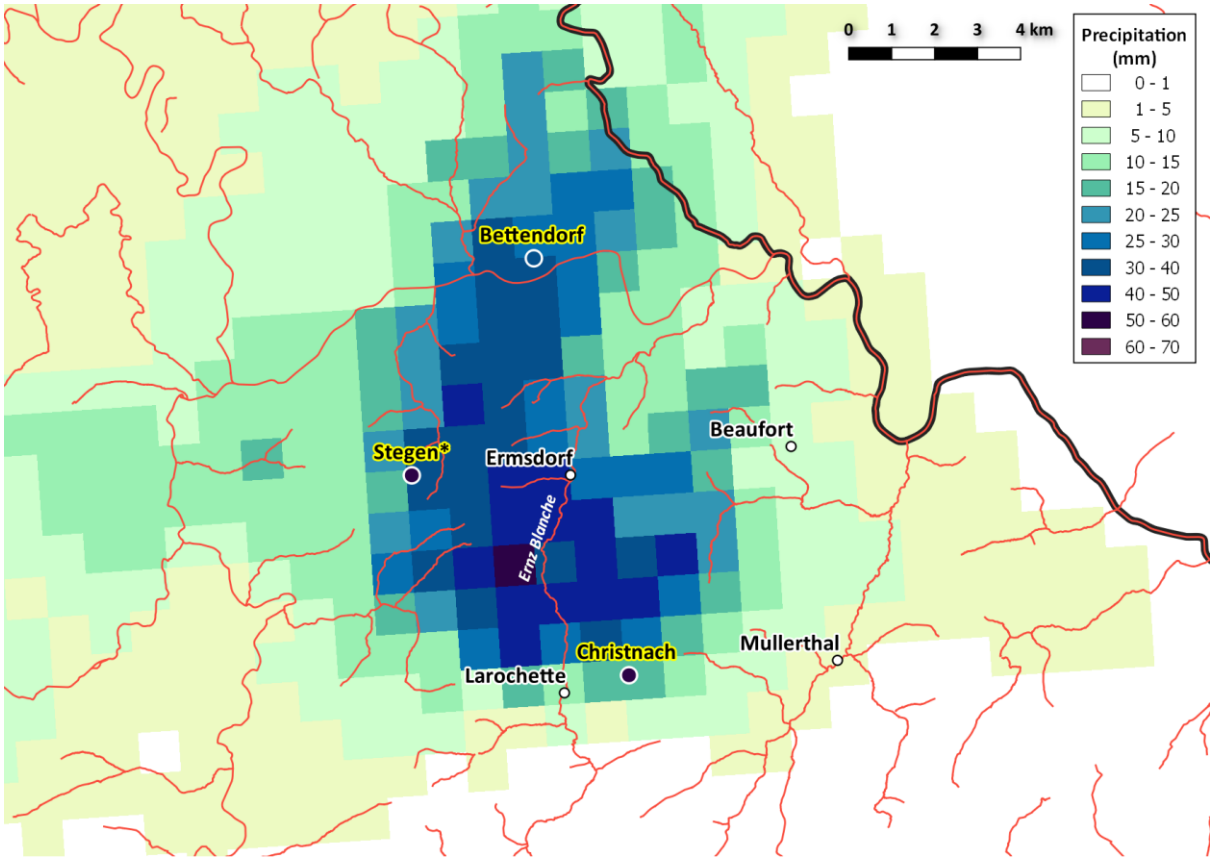

Figure 7. Accumulated precipitation (shaded; mm) between 17:50 and 18:50 UTC on 22 July 2016 in the study area, derived by RADOLAN-YW data (Winterrath et al. 2018) and measured by surface weather stations (towns with yellow text buffer; Bettendorf: 39.6 mm, Christnach: 53.1 mm, Stegen: 59.6 mm).

6. SUMMARY AND CONCLUSIONS

The 22 July Vallée de l'Ernz flash floods were investigated with regard to the synoptic-scale and mesoscale meteorological context focusing on the atmospheric ingredients of this event and on the characteristics of the storm as observed with radar and lightning data.

The large-scale atmospheric conditions were marked by weak pressure gradients. Strong latent instability and sub-synoptic-scale lifting mechanisms were sufficient to initiate thunderstorms over the Grand Duchy of Luxembourg on 22 July 2016. Furthermore, the radar analysis executed in this paper suggests that the merging of convective cells was most likely a crucial dynamical and microphysical process for the enhanced precipitation generation over the Vallée de l'Ernz, together with the presence of high total column atmospheric water vapour, weak lower- to mid-tropospheric kinematics and moderate upper-level shear. However, further research is needed to find out which atmospheric conditions favour the merging of convective cells and subsequent storm intensification, which could potentially cause major flooding. This severe weather event also highlights the importance of near-real time radar and lightning data with a high temporal and spatial resolution for operational nowcasting purposes.

The comparison of radar-based and in situ precipitation data revealed a striking underestimation by RADKLIM over the southern part of the Vallée de l'Ernz, where maximum rainfall amounts of 60 to 100 mm likely occurred between 17:50 and 18:50 UTC. The hydrological ingredients (e.g., soil moisture, land use, infiltration rate, surface runoff) have not been dealt with in this study, but they have been partially discussed by Pfister et al. (2018).

ACKNOWLEDGEMENTS

ECMWF's ERA5 reanalysis data is made available by the Copernicus Climate Change Service (https://cds.climate.copernicus.eu/). RADKLIM/RADOLAN data is accessible through DWD's open data portal (https://opendata.dwd.de/climate_environment/CDC/grids_germany/). The author thanks ASTA for providing archived weather station data (https://www.agrimeteo.lu/Agrarmeteorologie/Archiv/Orginalwerte). The author thanks the Kachelmann Group for archiving and visualizing operational radar data and making it freely available on its website (https://kachelmannwetter.com).

REFERENCES

Bartels, H., Weigl, E., Reich, T., Lang, P., Wagner, A., Kohler, O., and Gerlach, N. (2004): Projekt RADOLAN, Routineverfahren zur Online-Aneichung der Radar-niederschlags-daten mit Hilfe von automatischen Bodenniederschlagsstationen (Ombrometer). DWD, Offenbach, Germany, 111 pp. [Available online: https://www.dwd.de/DE/leis-tungen/radolan/radolan_info/abschlussbericht_pdf.pdf?__blob=publication-File&v=2]

Bennetts, D. A., Bader, M. J., and Marles, R. H. (1982). Convective cloud merging and its effect on rainfall. *Nature*, **300**, 42-45. DOI: https://doi.org/10.1038/300042a0

Betz, H.-D., Schmidt, K., Laroche, P., Blanchet, P., Oettinger, P., Defer, E., Dziewit, Z., and Konarski, J. (2009). LINET - an international lightning detection network in Europe. *Atmospheric Research*, **91**, 564-573. DOI: https://doi.org/10.1016/j.at-mosres.2008.06.012

Deierling, W., and Petersen, W. A. (2008). Total lightning activity as an indicator of updraft characteristics. *Journal of Geophysical Research*, **113**, D16210. DOI: https://doi.org/10.1029/2007JD009598

Doswell, C. A. III, Brooks, H. E., and Maddox, R. A. (1996). Flash flood forecasting: An ingredients-based methodology. *Weather and Forecasting*, **11**, 560-581. DOI: https://doi.org/10.1175/1520-0434(1996)011<0560:FFFAIB>2.0.CO;2

D'Letzeburger Land (1958). Ein Wolkenbruch seltenen Ausmaßes. [Available online: http://www.eluxemburgensia.lu/BnlViewer/view/index.html?lang=fr#pa-nel:pp|issue:1710926|article:DTL142|query:wolken-bruch]

Farnell, C., Rigo, T., and Pineda, N. (2017). Lightning jump as a nowcast predictor: application to severe weather events in Catalonia. *Atmospheric Research*, **183**, 130-141. DOI: http://dx.doi.org/10.1016/j.atmosres.2016.08.021

Fu, D., and X. Guo, (2006). A cloud-resolving study on the role of cumulus merger in MCS with heavy precipitation. *Advances in Atmospheric Sciences*, **23**, 857-868. DOI: https://doi.org/10.1007/s00376-006-0857-9

Fu, D., and Guo, X. (2012). A Cloud-Resolving Simulation Study on the Merging Processes and Effects of Topography and Environmental Winds. *Journal of Atmospheric Sciences*, **69**, 1232-1249. DOI: https://doi.org/10.1175/JAS-D-11-049.1

Hersbach, H., et al. (2020). The ERA5 global reanalysis. *Quarterly Journal of the Royal Meteorological Society,* **146**, 1999-2049. DOI: https://doi.org/10.1002/qj.3803

Jurković, P., Mahović, N., and Počakal, D. (2015). Lightning, overshooting top and hail characteristics for strong convective storms in Central Europe. *Atmospheric Research*, **161–162**, 153-168. DOI: https://doi.org/10.1016/j.atmosres.2015.03.020

Kreklow, J., Tetzlaff. B., Kuhnt, G., and Burkhard, B. (2019). A Rainfall Data Intercomparison Dataset of RADKLIM, RADOLAN, and Rain Gauge Data for Germany. *Data*, **4**, 118. DOI: https://doi.org/10.3390/data4030118

Luxemburger Wort (2018). Sturzflut 1958: Ein grausiges Schauspiel. [Available online: https://www.wort.lu/de/lokales/sturzflut-1958-ein-grausiges-schauspiel-5b36531b182b657ad3b8f3dc]

Mathias, L. (2019). Major flood event in the Mullerthal region on 1 June 2018: event analysis and predictability. Administration de la Navigation Aérienne, MeteoLux, 17 pp. [Available online: https://www.meteolux.lu/fr/produits-et-services/publications/]

Pfister, L., Faber, O., Hostache, R., Iffly, J. F., Matgen, P., Minette, F., Trebs, I., Bastian, C., Göhlhausen, D., Meisch, C., and Patz, N. (2018). Crue éclair du 22 juillet 2016 dans la région de Larochette. Luxembourg Institute of Technology, Esch-sur-Alzette, Luxembourg, 16 pp. [Available online: https://eau.gouvernement.lu/fr/services-aux-citoyens/publications/2021/brochures/Crue-eclair-du-22-juillet-2016.html]

Púčik, T., Groenemeijer, P., Rýva, D., and Kolář (2015). Proximity soundings of severe and non-severe thunderstorms in central Europe. *Monthly Weather Review*, **143**, 4805-4821. DOI: https://doi.org/10.1175/MWR-D-15-0104.1

Schultz, C. J., Petersen, W. A., and Carey, L. D. (2011). Lightning and severe weather: A comparison between total and cloud-to-ground lightning trends. *Weather and Forecasting*, **26**, 744-755. DOI: https://doi.org/10.1175/WAF-D-10-05026.1

Schultz, C. J., Carey, L. D., Schultz, E. V., and Blakeslee, R. J. (2017). Kinematic and microphysical significance of lightning jumps versus non jump increases in total flash rate. *Weather and Forecasting*, **32**, 275-288. DOI: http://dx.doi.org/10.1175/WAF-D-15-0175.1

Schumacher, R. S. (2017). Heavy rainfall and flash flooding. Oxford Research Encyclopedia of Natural Hazard Science. Oxford University Press, USA. DOI: https://dx.doi.org/10.1093/acrefore/9780199389407.013.132

Sinkevich, A. A., and Krauss, T. W. (2014). Changes in Thunderstorm Characteristics due to Feeder Cloud Merging. *Atmospheric Research*, **142**, 124-132. DOI: https://doi.org/10.1016/j.atmosres.2013.06.007

Sinkevich, A. A., Popov, V. B., Tarabukin, I. A., Dorofeev, E. V., Dovgalyuk, Y. A., Veremei, N. E., Mikhailovskii, Y. P., Snegurov, V. S., and Snegurov, A. V. (2018). Changes in Cu Characteristics and Precipitation during Cu Merging. *Russian Meteorology and Hydrology*, **43**, 506-515. DOI: https://doi.org/10.3103/S1068373918080022

Stein, A. F., Draxler, R. R., Rolph, G. D., Stunder, B. J. B., Cohen, M. D., and Ngan, F. (2015). NOAA's HYSPLIT Atmospheric Transport and Dispersion Modeling System. *Bulletin of the American Meteorological Society*, **96**, 2059-2077. DOI: https://doi.org/10.1175/BAMS-D-14-00110.1

Wapler, K. (2017). The life-cycle of hailstorms: Lightning, radar reflectivity and rotation characteristics. *Atmospheric Research*, **193**, 60-72. DOI: https://doi.org/10.1016/j.atmosres.2017.04.009

Westcott, N.E. (1984). A historical perspective on cloud mergers. *Bulletin of the American Meteorological Society*, **65**, 219-227. DOI: https://doi.org/10.1175/1520-0477(1984)065%3C0219:AHPOCM%3E2.0.CO;2

Westcott, N.E. (1994). Merging of convective clouds: cloud initiation, bridging, and subsequent growth. *Monthly Weather Review*, **122**, 780-790. DOI: https://doi.org/10.1175/1520-0493(1994)122%3C0780:MOCCCI%3E2.0.CO;2

Winterrath, T., Brendel, C., Hafer, M., Junghänel, T., Klameth, A., Walawender, E., Weigl, E., and Becker, A. (2017). Erstellung einer radargestützten Niederschlagsklimatologie, Abschlussbericht, Berichte des Deutschen Wetterdienstes, Nr. 251. [Available online: https://www.dwd.de/DE/leistungen/pbfb_verlag_berichte/pdf_einzelbaende/251_pdf.pdf?__blob=publicationFile&v=2]

Winterrath, T., Brendel, C., Hafer, M., Junghänel, T., Klameth, A., Lengfeld, K., Walawender, E., Weigl, E., and Becker, A. (2018). RADKLIM Version 2017.002: Reprozessierte, mit Stationsdaten angeeichte Radarmessungen (RADOLAN), 5-Minuten-Niederschlagsraten (YW). DOI: 10.5676/DWD/RADKLIM_YW_V2017.002